VIRTUAL EXPERIMENTAL STUDY OF MICROSTRUCTURE DESIGN OF DUAL PHASE STEEL FOR OPTIMAL FORMABILITY

Y.G. AN[1], W.D.T. SPANJER[2], P.J.J. KOK[3]

Application and Engineering, Research and Development, Tata Steel in Europe,
1970 CA IJmuiden, the Netherlands,
[1]yuguo.an@tatasteel.com, [2]wil.spanjer@tatasteel.com, [3]piet.kok@tatasteel.com

Key words: Dual phase steel, Virtual experiment, formability.

Abstract. The highly competitive automotive market demands both lightweight and safe vehicles. These requirements can be met using advanced high strength steels. Dual phase steels are widely used in automotive applications for structural parts and crash columns because of their high strength, high work hardening index and reasonable ductility. In this research, the plastic behaviour and formability of dual phase steels are analysed and correlated with microstructure via virtual experiments. Different virtual dual phase microstructures were generated for this study, composed of a highly formable ferrite steel matrix with different volume fractions of martensite. The work hardening, plastic anisotropy, yield loci and formability performance are analysed using virtual experimentation. The results indicate that the strength of dual phase steels increases with increasing volume fraction of martensite. The plastic anisotropy r-value of dual phase steels is dominated by the ferrite texture but it decreases with an increasing amount of martensite, particularly when the volume fraction is greater than 20%. The presence of martensite reduces deep drawing formability in general. However, it increases the stretching factor and the maximum value is reached when the martensite fraction is in the range 10-20%. It is concluded that a good formability of dual phase steel is possible if the volume fraction of martensite is low and the γ-fibre texture of ferrite is strong.

1 INTRODUCTION

The highly competitive automotive market demands lightweight and safe vehicles. These requirements can be met using different types of high strength steels [1]. Dual phase steel is a low carbon and low alloy steel, usually consisting of 10-50% martensite in a ductile ferrite matrix. It is widely used for structural parts and crash columns because of the high strength-to-weight ratio, low yield-to-ultimate strength ratio and reasonably good ductility [2-6]. Another important application for sheet metals is automotive outer panels, which are commonly made out of highly formable IF steel or bake hardening steels. Advanced high strength steels have not been used for the outer panels due to the high formability required to achieve complex geometries. To explore the possible application of dual phase steels for automotive outer panels in order to achieve weight reduction, it is necessary to study the formability potential and limitations of this type of steel as a function of microstructure. In this research, a range of dual phase steels have been generated virtually, consisting of a ferrite matrix of highly formable steel and containing different volume fractions of martensite. The work hardening behaviour, plastic anisotropy, yield loci and formability performance are analysed using representative volume

element (RVE). The virtual experiments were simulated using the polycrystal plasticity code DAMASK [7].

2 MATERIALS AND VIRTUAL PLASTICITY TESTS

2.1 Highly formable steel and dual phase steels

The formability demand for outer panels is high due to the complex geometry of the parts and high deformation levels. Conventionally, highly formable IF sheet steels or bake hardening steels are used for outer panels. Following this philosophy, the texture of the ferrite matrix can be represented by the texture of a DC06 sheet, which is similar to that of DX56. The measured ODF of this material is shown Fig. 1. It is known that the strong γ–fibre is helpful for deep drawing formability. At present no dual phase steel with such a strong γ–fibre has been manufactured by steel producers. However, the potential to produce dual phase steel with strong anisotropy is possible and this has been demonstrated elsewhere [8]. So in this study, different virtual dual phase steels were generated using DC06 to represent the ferrite matrix and different volume fractions of martensite were added.
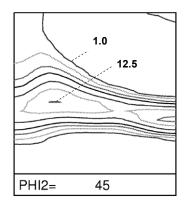

Figure 1. The ODFs of the DC06 material at PHI2= 45º section with contour levels of 0.7 _1.0 _1.4 _2.0 _2.8 _4.0 _5.6 _8.0 _11.0 _16.0.

2.2 Virtual plasticity testing for work hardening and yield locus

Work hardening behaviour is conventionally measured by uniaxial tensile testing. The measured flow stress behaviour and the plastic anisotropy *r*-values are used to define certain analytical yield functions [9]. In order to define the yield loci more precisely, several other plasticity tests, such as the through-thickness compression test, the plane strain tension and the simple shear test, were developed by Tata Steel to give more measured data points in several different stress and strain states [10-12]. An accurate description of the yield locus can be obtained by Vegter interpolation over the tests [13]. For the dual phase steels, virtual plasticity experiments simulating the uniaxial tension, plane strain tension, through thickness compression and simple shear were carried out as illustrated in Fig.2.

To validate the RVE model, through-thickness compression testing of the highly formable steel was conducted, as shown in Fig. 3. The detailed experimental procedure is described elsewhere [11]. The work hardening measured in this compression test was compared with the RVE simulation, as discussed in the next section.
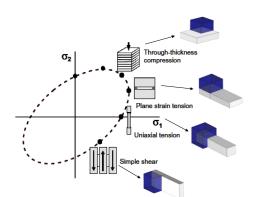
Figure 2. Illustration of different plasticity tests for data points on yield locus. The blue and grey blocks refer to sample geometry before and after deformation.
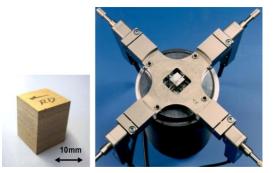

Figure 3. Stacked specimen and extensometer used in the compression test. The displacements in the RD and TD are measured for the calculation of strains.

3   POLYCRYSTAL PLASTICITY MODEL AND RVE SIMULATION

3.1 Polycrystal plasticity model

The polycrystal plasticity model used in the present study is an adoption of the phenomenological description for body-centered cubic crystals incorporated in the Damask framework [14-16]. The microstructure is parameterised in terms of a slip resistance g^α on each of the slip systems. These resistances evolve asymptotically towards g^∞ with shear according to the following relationship;

$$\dot{g}^\alpha = \dot{\gamma}^\beta h_0 \left| 1 - g^\beta / g_\infty \right|^a \operatorname{sgn}(1 - g^\beta / g_\infty) h_{\alpha\beta} \tag{1}$$

with parameters h_0 and a. The interaction between different slip systems is captured by the hardening matrix $h_{\alpha\beta}$. Given a set of current slip resistances, shear on each system occurs at a rate;

$$\dot{\gamma}^\alpha = \dot{\gamma}_0 \left| \tau^\alpha / g^\alpha \right|^n \operatorname{sgn}(\tau^\alpha) \tag{2}$$

with γ_0 as reference shear rate, $\tau^\alpha = S * (b^\alpha \otimes n^\alpha)$, and n the stress exponent. The superposition of shear on all slip systems in turn determines the plastic velocity gradient;

$$L_p = \dot{\gamma}^\alpha b^\alpha \otimes n^\alpha \qquad (3)$$

where b^α and n^α are unit vectors along the slip direction and slip plane normal, respectively.

3.2 Parameters for the constitutive material model

In the DAMASK software, the texture is easily introduced with the texture component method for the representation of statistical textures. The texture is measured by X-ray diffraction method and presented in the form of the orientation distribution function (ODF). The hardening parameters in slip system for the virtual testing are calibrated on the basis of work hardening in uniaxial tensile tests in the rolling direction. This leads to the hardening parameters given in table 1 for ferrite. For martensite, the parameters used are based on literature references. The quality of the model prediction is evaluated by comparing simulations to the corresponding experimentally measured stress-strain responses in the through-thickness compression- and uniaxial tensile tests conducted on the highly formable steel sheet.

Table 1: Material parameters; elastic constants C_{ab}, reference shear rate $\dot{\gamma}_0$, stress exponent n, initial and saturation flow stress τ_0 and τ_∞, hardening parameters $h0$.

parameter	Ferrite	martensite
c11	233.3e9	417.4e9
c12	135.5e9	242.4e9
c44	118.0e9	211.1e9
$\dot{\gamma}_0$	0.001	0.001
n	20	20
τ_0	43.58e6	332.0e6
τ_∞	203.5e6	714.0e6
h_0	1518.0e6	563.0e9

3.3 RVE and Boundary conditions

The virtual specimen is a representative volume element of real material. The material consists of many differently oriented grains. Grains undergo plastic deformation due to displacement on slip planes along preferred slip direction; in each crystal 24 slip systems for bcc are used. Slip systems are considered active if the critical shear stress is exceeded. This critical shear stress corresponds to the yield curve of empirical model. As the parameters are determined from simple tensile tests the hardening coefficient of all 24 bcc slip systems are assumed to be identical. This is close to the pencil glide model, where the slip direction is restricted to the <111> and the slip planes are those with the highest resolved shear stress.

A periodic cubic volume element is constructed from a Voronoi tessellation of randomly placed seed points [7,17]. The crystal orientation of each grain is assigned according to the ODF measured by X-ray diffraction. The martensite, which is finer than the ferrite grains, distribute randomely. A RVE for dual phase steels consisting of 512 grains with 20% martensite in volume fraction is illustrated in Fig.4.

The boundary conditions chosen for RVEs to construct yield locus were as follows; the

uniaxial tension, plane strain tension, through-thickness compression and simple shear. The uniaxial tension and plane strain tension were performed in the rolling direction (RD), transverse direction (TD) and 45° to the RD. The simple shear tests were conducted in the RD and 45° to the RD. The through-thickness compression was in the sheet normal direction.
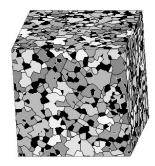

Figure 4. RVE with 20% martensite (black) in volume fraction

4   RESULTS AND DISCUSSION

4.1   Validation of the RVE model for DC06 in the through-thickness compression

The work hardening behaviour of the DC06 material was measured in the uniaxial tensile test and through thickness compression test. The measured work hardening data in the tensile test in the rolling direction was used to fit material parameters for the RVE. The through-thickness compression test was carried out at similar strain rate to the tensile test and the measured work hardening was compared with the RVE simulations as a validation exercise.

RVE simulations for the uniaxial tension and through-thickness compression were carried out using parameters listed in table 1. The texture of the DC06 was discretized for the RVE. The load cases for the uniaxial tension along rolling direction and through-thickness compression along sheet normal are prescribed through the boundary conditions in (4) and (5), respectively.

$$\frac{\dot{\overline{F}}}{10^{-3}s^{-1}} = \begin{vmatrix} 1 & * & * \\ 0 & * & * \\ 0 & 0 & * \end{vmatrix}, \qquad \frac{\overline{P}}{Pa} = \begin{vmatrix} * & 0 & 0 \\ * & 0 & 0 \\ * & * & 0 \end{vmatrix} \tag{4}$$

$$\frac{\dot{\overline{F}}}{10^{-3}s^{-1}} = \begin{vmatrix} * & * & * \\ 0 & * & * \\ 0 & 0 & -1 \end{vmatrix}, \qquad \frac{\overline{P}}{Pa} = \begin{vmatrix} 0 & 0 & 0 \\ * & 0 & 0 \\ * & * & * \end{vmatrix} \tag{5}$$

The stress strain curves in the uniaxial tension in the RD and the uniaxial compression in the ND measured in the experiments and calculated from the RVE simulations are plotted in Fig.5. The results in Fig.5 indicate that the predicted work hardening fits well with the measured stress and strain curves for both the tensile test and the through-thickness compression test. So the RVE model is validated for the DC06, and this approach is used further with confidence for dual phase steels.
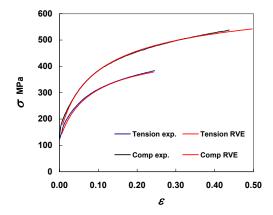
Figure 5. Measured work hardening in tensile test and through-thickness compression test and the modelled ones from RVE simulations.

4.2 The work hardening of dual phase steels

The effect of the second phase on the flow stress of dual phase steels was modelled using RVE simulation of the tensile test in the rolling direction, as shown in Fig. 6. With increasing volume fraction of martensite, the flow stress is significantly increased. At a volume fraction of around 20%, the tensile strength reaches approximately 450MPa; this is a desirable strength level for outer panel applications.

Another remarkable effect of martensite on strength is that it has less effect on the yield strength than on the tensile strength. Fig. 7 shows the calculated work hardening rate, $\delta\sigma/\delta\varepsilon$, against major strain in tensile test. The graph indicates clearly that the work hardening rate increases with increasing volume fraction of martensite at the onset of plastic deformation. However, this enhanced work hardening rate due to second phase declines with straining, and at strains larger than 5%, the difference in work hardening becomes negligible. Experimentally it is well known that dual phase steels show low yield strength but high work hardening index in comparison with other steel grades. Results in Fig. 6 and Fig. 7 clearly capture this work hardening character of dual phase steels.
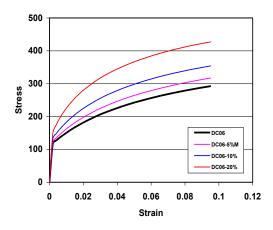

Figure 6. Simulated work hardening curves for the dual phase steels containing different volume fractions of martensite.
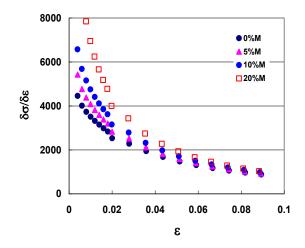
Figure 7. Calculated work hardening rate against strain for the dual phase steels containing different volume fraction of martensite.

4.3 Plastic anisotropy *r*-value of dual phase steels

The plastic anisotropy *r*-value measured in the tensile test is another important formability parameter for deep drawing. The calculated *r*-value profile for the DC06 and dual phase steels are plotted in Fig. 8. When the volume fraction of martensite is low, e.g. 5% martensite, the *r*-value profile is improved to some extent, particularly the planar anisotropy is reduced. With increasing volume fraction of martensite, the *r*-value in the rolling direction drops continuously. At 20% martensite, the *r*-value profile becomes significantly lower than that of DC06 in all directions.

In addition to the conventionally defined r-value profile, the evolution of *r*-value with straining also influences forming performance, as shown elsewhere [18]. The incremental *r*-value with straining in the rolling direction for the DC06 and dual phase steel containing 20% martensite is shown in Fig.9. Clearly, the martensite stabilizes the *r*-value evolution, although the value at small strains is lower than the *r*-value of the ferrite matrix.
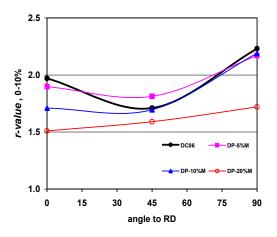

Figure 8. Simulated *r*-value profile of the DC06 and dual phase steels with different volume fraction of martensite.
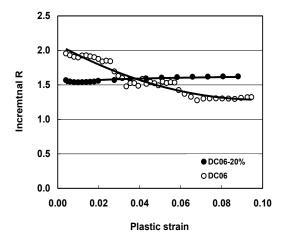
Figure 9. Evolution of incremental *r*-value with straining for the DC06 and dual phase steel with 20% martensite in RVE simulation.

4.4 Effect of martensite volume fraction on yield loci and formability

The yield locus is an important part of a constitutive material model. The boundary conditions chosen for RVEs in the construction of the yield locus were uniaxial tension, plane strain tension, through-thickness compression and simple shear. Based on the calculated work hardening data from the RVE simulations in different strain states, the yield locus can be established in different sections relative to the rolling direction. Fig. 10 shows the yield loci of the DC06 and the dual phase steels in the RD-TD section. It is observed that the shape of the yield loci contracts in the biaxial stretching direction with increasing volume fraction of martensite, whilst expanding very slightly in the shear regime, leading to changes in the formability in general. The yield loci are based on work hardening data in a certain strain range, and we know that the yield loci evolve with straining due to evolution of texture as demonstrated elsewhere [18]. To have a more complete and precise overview of the effect of martensite on formability, it is convenient to study the relationship of the deep drawing factor and the stretching factor with deformation at different volume fractions of martensite.
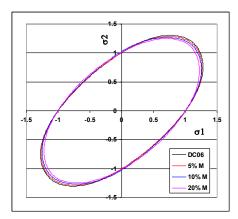

Figure10. Yield loci calculated from RVE for DC06 and dual phase steels with different volume fraction of Martensite in the RD-TD section.

Usually the deep drawing and stretching factor are two parameters taken from yield loci as follows,

$$DDR = f_p/f_s \tag{6}$$

$$STR = f_p/f_b \tag{7}$$

Here f_p, f_b and f_s refer to the major stress factor of the plane strain point, biaxial point and shear point, respectively, on the yield locus. Because of the evolution of yield loci with deformation, the two formability factors also vary with straining. So we define here an instantaneous deep drawing factor, *DDRi*, and stretching factor, *STRi*, using the following formula,

$$DDRi = \sigma_p/\sigma_s \tag{8}$$

$$STRi = \sigma_p/\sigma_b \tag{9}$$

Here σ_p, σ_b and σ_s refer to flow stress at the same equivalent strain in plane strain, biaxial and shear state, respectively. The instantaneous deep drawing factor and stretching factor with straining are plotted in Fig.11 and Fig. 12, respectively.
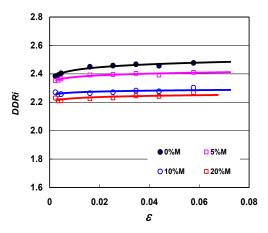
Figure11. Instantaneous deep drawing factor with straining for DC06 and dual phase steels.
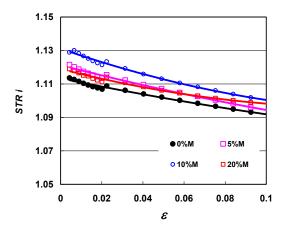
Figure12. Instantaneous stretching factor with straining for DC06 and dual phase steels.

The deep drawing factor is an important parameter when performing deep drawing operations. For DC06, the instantaneous deep drawing factor increases slightly with straining and then saturates at a value close to 2.5. For dual phase steel with different volume fractions of martensite, the trend of *DDRi* with straining is similar to the DC06, but the *DDRi* level decreases with an increasing amount of martensite. This trend can be seen also from the yield loci on which the shear factor increases, while the plane strain factor decreases, with increasing amounts of martensite, leading to a decrease in the deep drawing factor.

Stretching formability is influenced by the stretching factor. For highly formable DC06 steel, the stretching factor declines continuously with strain, as shown in Fig.12. For dual phase steels, the trend of *STRi* with straining is similar, but the level of *STRi* depends on the volume fraction of martensite. At volume fraction of 5% and 10% martensite, the stretching factor is enhanced with an increasing amount of martensite. However, at 20% martensite, the stretching factor drops to the level of dual phase steel with volume fraction of 5% martensite. So the optimum stretching factor may lie in the range of 10-20% martensite in dual phase steels.

In summary, the deep drawing formability of dual phase steels is reduced by the presence of martensite, in comparison with DC06. The stretch formability is improved, reflected in the increased stretching factor, although the effect of martensite on ductility has to be taken into account when stretching formability is considered.

5   CONCLUSIONS

- The strength of dual phase steels increases with increasing volume fraction of martensite. The plastic anisotropy *r*-value of dual phase steels is dominated by the texture of ferrite, and decreases with increasing amount of martensite. The *r*-value profile is strongly reduced at martensite volume fraction of 20%.
- The formability of dual phase steels is different in character than that of ferrite DC06. The martensite present reduces the deep drawing factor and therefore deep drawing formability in general. However, martensite increases the stretching factor and the maximum value is reached in the range of 10- 20% martensite.
- Dual phase steel with good formability is possible when the volume fraction of martensite is in the range of 10-20%, and the γ-fibre texture of the ferrite matrix is strong.

6. REFERENCES

[1]. E. De Moor, P. J. Gibbs, J. G. Speer, D. K. Matlock and J. G. Schroth, "Strategies for third generation advanced high-strength steel development", *AIST Transactions, Iron & Steel Technology Transactions*, (2010), vol. 7, pp. 133-144.
[2]. Furukawa T, Tanino M, Morikawa H. Endo, Effects of Composition and Processing Factors on the Mechanical Properties of As-hot-rolled Dual-phase Steels, *M Trans ISIJ* (1984); 24:113.
[3]. R.G. Davies, Influence of martensite composition and content on the properties of dual phase steels, *Metall.Trans*.A9 (1978), 671–679.
[4]. Kim NJ, Thomas G., Effects of morphology on the mechanical behavior of a dual phase Fe/2Si/0.1C steel, *Metall Trans* A, (1981);12A:483.

[5]. Nakagawa AH, Thomas G., Microstructure-mechanical property relationships of dual-phase steel wire, *Metall Trans* A, (1985);16A:831.

[6]. Kadkhodapour J, Schmauder S, Raabe D, Ziaei-Rad S, Weber U, Calcagnotto M., Experimental and numerical study on geometrically necessary dislocations and non-homogeneous mechanical properties of the ferrite phase in dual phase steels, *Acta Mater,* (2011); 59:4387.

[7]. DAMASK: the Düssendorf Advanced Material Simulation Kit, http://damask.mpie.de/Home/WebHome, (2016).

[8]. H.Hu, Studies on the development of high strength dual phase steel sheets with high rm values. *Metal. Trans* A, (1982), 13A, 1257.

[9]. Hill, R., A theory of the yielding and plastic flow of anisotropic metals. *Proceedings of the Royal Society London* A, (1948),193, 281–297.

[10]. An, Y.G., Vegter, H., Elliott, L., A novel and simple method for the measurement of plane strain work hardening. *Journal of Materials Processing Technology,* (2004), 155–156, 1616–1622.

[11]. An, Y.G., Vegter, H., Analytical and experimental study of frictional behaviour in through-thickness compression test. *Journal of Material Processing Technology,* (2005), 160, 148–155.

[12]. An, Y.G., Vegter, H., Heijne, J., Development of simple shear test for the measurement of work hardening. *Journal of Materials Processing Technology* (2009), 209, 4248–4254.

[13]. Vegter, H., van den Boogaard, A.H., A plane stress yield function for anisotropic sheet material by interpolation of biaxial stress states. *International Journal of Plasticity* (2006), 22, 557–580.

[14]. D. Peirce, R. J. Asaro, and A. Needleman. Material rate dependence and localized deformation in crystalline solids. *Acta Metall.,* (1983), 31:1951–1976.

[15]. Hutchinson, J.W., Bounds and self-consistent estimates for creep of polycrystalline materials. Proc. Roy. Soc. (1976), A 348, 101–127.

[16]. F. Roters, P. Eisenlohr, C. Kords, D. D. Tjahjanto, M. Diehl, D. Raabe, DAMASK: the D¨usseldorf Advanced Material Simulation Kit for studying crystal plasticity using an FE based or a spectral numerical solver, *Procedia IUTAM 3* (2012) 3 − 10.

[17]. P.J.J.Kok, W. Spanjer, H. Vegter, A microstructure based model for the mechanical behaviour of multiphase steels, *Key Engineering Materials,* (2015), Vols. 651-653 p 975.

[18]. Y.G. An, H. Vegter, S. Melzer, P. Romano Triguero, Evolution of the plastic anisotropy with straining and its implication on formability for sheet metals, *Journal of Materials Processing Technology*, (2013), 213, 1419–1425.